

## Numerical study of trailing edge cooling in a gas turbine blade

Pilaisiri Thongsanit<sup>1)</sup> and Theeradech Mookum<sup>2)</sup>

<sup>1), 2)</sup> School of Science, Mae Fah Luang University, Chiang Rai 57100, Thailand  
<sup>2)</sup> [theeradech@mfu.ac.th](mailto:theeradech@mfu.ac.th)

### ABSTRACT

A realistic trailing edge cooling system is very high pressure in a gas turbine blade. The internal cooling of the first stage gas turbine blade is required to enhance turbulence and heat transfer. This work presents a numerical investigation to study the cooling effectiveness in a gas turbine blade with different trailing edge injection. The bottom inlet and lateral inlet are designed in the trailing edge region. The numerical simulation is based on the Reynold Average Navier-Stoke equations coupled with the heat equation. The numerical results show that the average velocity magnitude of the cooling air passing through the trailing cavity from the bottom is higher than that from the lateral wall and both cases produce the same level of the average cooling effectiveness on the trailing edge region.

### 1. INTRODUCTION

Gas turbine is a hot gas path component in combustion section operating at high temperature up to 1500 °C. The degradation of the turbine increases with increasing inlet temperature (Yoshioka 1986). This leads to the blade failure especially in the trailing edge region due to the thin shape and high pressure. It is essential to cool the blade externally and internally. The internal cooling is passing the coolant through several enhanced serpentine passages inside the blades and extracting the heat from the outside of the blades.

The trailing edge cooling technology has been carried out by a number of research works. The experimental study was conducted by Yang and Hu (Yang 2012) investigating the flow characteristics on the trailing edge region. The trailing edge was designed as five-slot ejection. Pressure sensitive paint (PSP) technique was used to measure the cooling effectiveness. Becchi et al. (Becchi 2015) measured film cooling effectiveness of three trailing edge configurations: five exit slots and no film hole, five exit slots and a single row of film holes, and no exit slot and three rows of film holes.

Their results showed that at the exit, the shape with five exit slots and a single row of film holes presents the high level of the cooling effectiveness.

Most of trailing edge cooling schemes were focused on shapes, dimples/rib turbulators, coolant ejections, and coolant injections. Cunha et al. (Cunha 2006) presented the trailing edge heat transfer in four configurations: solid wedge shape without discharge, wedge with slot discharge, wedge with discrete-hole discharge, and wedge with pressure-side cut-back slot discharge. They found that the cut-back design had more effective temperature distribution than the others. Shen et al. (Shen 2016) studied the heat transfer performance in the trailing edge rectangular and trapezoidal cooling passages with dimples and ejection slots. The conclusions were obtained that the trapezoidal channel with dimples enhances the heat transfer from 30% - 70%. Siddique et al. (Siddique 2015) confirmed that the inline dimples with the value of depth to diameter ratio 0.25 should be used to enhance the heat transfer performance.

The trailing edge coolant ejection was also studied on many models. Taslim et al. (Taslim 2011, 2013) studied the effects of exit slots on the heat transfer in the cross-over jet impingement for the trailing-edge cooling cavities. The exit slots were designed as inline and staggered flow arrangements. They concluded that both cases produced the same level of heat transfer. Effendy et al. (Effendy 2016) evaluated the cooling performance of trailing-edge cutback using detached-eddy simulation (DES) method with various lip thickness to slot height ratios ( $t/H$ ). It was observed that increasing the  $t/H$  ratio leads to the decrease of film-cooling effectiveness.

The cooling schemes by injecting the cooling air through the trailing edge was studied. The injection via the impingement holes installed at lateral wall was conducted by Chung et al. (Chung 2014). The thermal performance of four different blockage configurations for gas turbine blade cooling near the trailing edge was investigated. It is noted that the inclined blockage can improve the cooling performance higher than baseline design. Deng et al. (Deng 2018) proposed the experimental study of two-inlet cooling from bottom and lateral of the trailing edge region and compared the heat transfer performance with single-inlet cooling. It was found that the lateral-inlet cooling presented the better heat transfer than bottom-inlet and two-inlet cases.

This work focuses on the numerical experiment to study the turbulence flow and the cooling effectiveness on the trailing edge. Two different inlet injections are designed, including bottom inlet and lateral inlet. The Reynold Average Navier-Stoke (RANS) equations and the heat equation are studied to visualize the numerical results.

## 2. NUMERICAL ANALYSIS

### 2.1 Governing equations for the fluid

In this work, we adopted the Reynolds stress model based on the RANS equations. The flow is assumed to be turbulent and incompressible. The governing equations for the air consist of the continuity equation, momentum equation, and energy equation as follows:

$$\frac{\partial}{\partial x_i} (\rho_{air} u_i) = 0, \quad (1)$$

$$\frac{\partial}{\partial x_i} (\rho_{air} u_i u_j) = -\frac{\partial P}{\partial x_j} + \frac{\partial}{\partial x_i} \left[ \mu_{air} \left( \frac{\partial u_j}{\partial x_i} + \frac{\partial u_i}{\partial x_j} \right) - \rho_{air} \overline{u'_i u'_j} \right], \quad (2)$$

and

$$\frac{\partial}{\partial x_i} (\rho_{air} c_{p,air} u_i T) = \frac{\partial}{\partial x_i} \left[ \lambda_{air} \frac{\partial T}{\partial x_i} - \rho_{air} c_{p,air} \overline{u'_i T'} \right], \quad (3)$$

where  $u_i$  is the velocity in the  $x_i$  direction,  $P$  the pressure,  $\rho_{air}$  the density of air,  $\mu_{air}$  the dynamic viscosity of air,  $T$  the temperature,  $c_{p,air}$  the heat capacity of air, and  $\lambda_{air}$  the thermal conductivity of air.

## 2.2 Turbulence model

The Reynolds stress  $-\rho_{air} \overline{u'_i u'_j}$  and the turbulent heat flux  $-\rho_{air} \overline{u'_i T'}$  in the equations (2) and (3) are defined based on the Boussinesq eddy-viscosity assumption respectively as Eq. (4).

$$-\rho_{air} \overline{u'_i u'_j} = \mu_t \left( \frac{\partial u_j}{\partial x_i} + \frac{\partial u_i}{\partial x_j} \right) - \frac{2}{3} \rho_{air} k \delta_{ij} \quad (4)$$

and

$$-\rho_{air} \overline{u'_i T'} = \frac{\mu_t}{Pr_t} \frac{\partial T}{\partial x_i}, \quad (5)$$

where  $Pr_t$  the turbulent Prandtl number, and  $\delta_{ij}$  the kronecker delta function. The turbulent viscosity is defined as Eq. (6).

$$\mu_t = \rho_{air} C_\mu \frac{k^2}{\varepsilon}. \quad (6)$$

The standard  $k - \varepsilon$  model is used to solve the turbulence kinetic energy  $k$  and its dissipation rate  $\varepsilon$ , which are modeled as Eq. (7), Eq. (8).

$$\frac{\partial}{\partial x_j} (\rho_{air} k u_j) = \frac{\partial}{\partial x_j} \left[ \left( \mu_{air} + \frac{\mu_t}{\sigma_k} \right) \frac{\partial k}{\partial x_j} \right] + G_k - \rho_{air} \varepsilon, \quad (7)$$

$$\frac{\partial}{\partial x_j} (\rho_{air} \varepsilon u_j) = \frac{\partial}{\partial x_j} \left[ \left( \mu_{air} + \frac{\mu_t}{\sigma_\varepsilon} \right) \frac{\partial \varepsilon}{\partial x_j} \right] + C_{1\varepsilon} \frac{\varepsilon}{k} G_k - C_{2\varepsilon} \rho_{air} \frac{\varepsilon^2}{k}. \quad (8)$$

where  $G_k = -\rho_{air} \overline{u'_i u'_j} \frac{\partial u_j}{\partial x_i}$  is the production of turbulent kinetic energy. The model constants are as follow Launder (1974) and Kays (1994):

$$C_{1\varepsilon} = 1.44, C_{2\varepsilon} = 1.92, C_\mu = 0.09, \sigma_k = 1.0, \sigma_\varepsilon = 1.3, \text{ and } Pr_t = 0.85.$$

## 2.3 Heat transfer in solid region

The steady state heat equation in the turbine blade (solid region) has the following form:

$$\frac{\partial}{\partial x_i} \left( \lambda_s \frac{\partial T}{\partial x_i} \right) = 0 \quad (9)$$

where  $\lambda_s$  represents the thermal conductivity of the solid.

# 3. COMPUTATIONAL METHODOLOGY

## 3.1 Computational domains

The computational domain for the blade of two channels with a  $45^\circ$  angle ribbed wall configured with tip holes is shown in Fig. 1. The first channel connects to leading part via 10 impinging holes of 0.001 m in diameter. The second channel connects to trailing part via 10 impinging holes of 0.001 m in diameter. Each channel has ribs on two opposite walls with  $45^\circ$  angle ribbed. Rib height is 0.0014 m and pitch length is 0.011 m. The tip cap has 9 holes with a diameter of 0.003 m. The full blade has a thickness of 0.0015 m, a length of 0.09189 m, a width of 0.04516 m, and a height of 0.12331 m with two cooling air flow from the root.

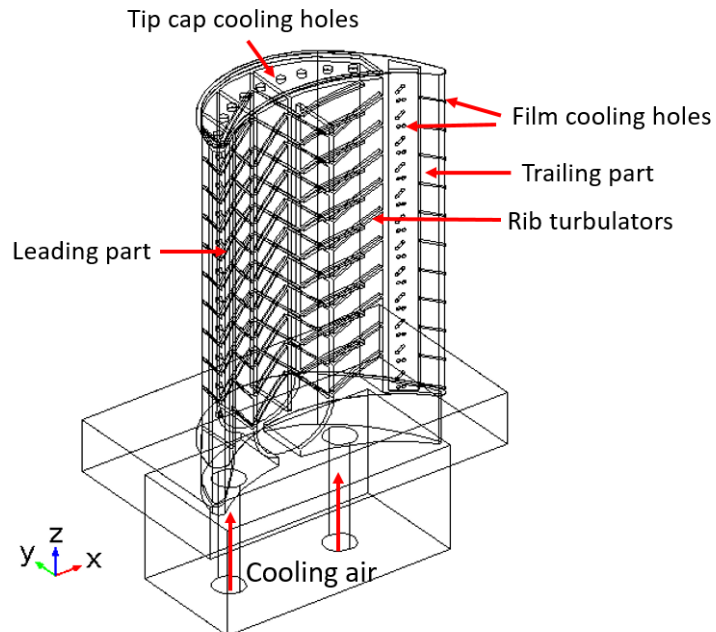


Fig. 1 Computational domains

### 3.2 Model description for trailing edge cooling geometry

The smooth channel trailing edge is cooled by the film cooling and coolant injection. There are three rows of film cooling holes, one row each on the trailing edge, pressure side, and suction side. Twelve holes on both pressure and suction side are parallel with upward angle of  $45^\circ$  and eleven of  $90^\circ$  holes are arranged on the trailing edge. Fig. 2 shows trailing injection configurations for two different cases. Case 1 depicts the bottom inlet injection. The cooling air passes through the trailing cavity from the bottom. Case 2 illustrates the lateral inlet injection. The cooling air passes through the trailing cavity from the channel wall.

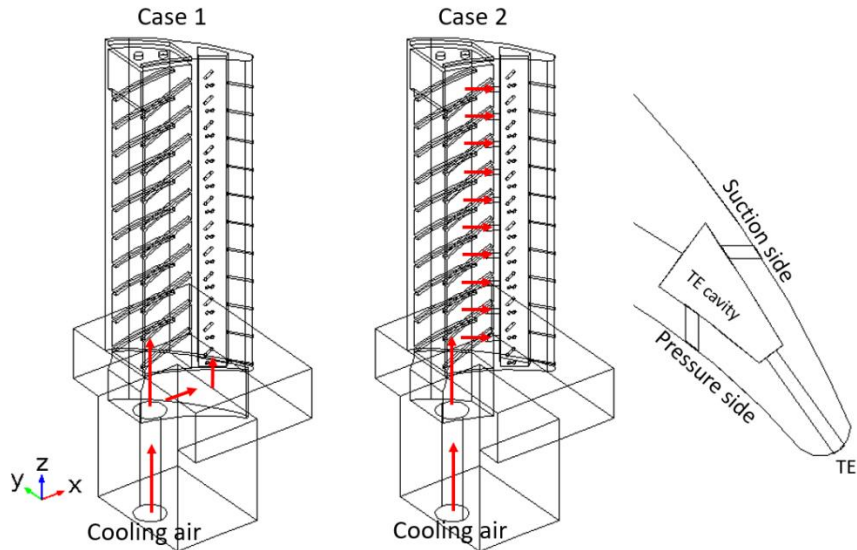


Fig. 2 Trailing edge cooling geometry

### 3.3 Numerical method

In this study, the three-dimensional mathematical model is implemented into the software COMSOL Multiphysics. The cooling air temperature  $T_c = 400^\circ\text{C}$  is injected into the blade with the inlet velocity  $U_{in} = 70 \text{ m/s}$ , the inlet turbulent kinetic energy  $k_{in} = 0.005 \text{ m}^2/\text{s}^2$ , and inlet turbulent dissipation rate  $\varepsilon_{in} = 0.00548 \text{ m}^2/\text{s}^3$ . The mainstream temperature from the combustion chamber is  $T_\infty = 1200^\circ\text{C}$ . The physical properties of air and solid material (Inconel 718) related to a function of temperature are shown in table 1.

Table 1. Physical properties of air and solid (Inconel 718).

---

Density of air,  $\rho_{air}$ , [ $\text{kg}/\text{m}^3$ ]

$$352.7T^{-1}$$

Specific heat capacity of air,  $c_{p,air}$ , [ $\text{J}/(\text{kg.K})$ ]

$$1093 - 0.6356T + 1.634 \times 10^{-3}T^2 - 1.413 \times 10^{-6}T^3 + 5.595 \times 10^{-10}T^4 - 8.663 \times 10^{-14}T^5$$

Dynamic viscosity of air,  $\mu_{air}$ , [ $\text{kg}/(\text{m.s})$ ]

$$3.893 \times 10^{-6} + 5.754 \times 10^{-8}T - 2.676 \times 10^{-11}T^2 + 9.710 \times 10^{-15}T^3 - 1.356 \times 10^{-18}T^4$$

Thermal conductivity of air,  $\lambda_{air}$ , [ $\text{W}/(\text{m.K})$ ]

$$-8.404 \times 10^{-4} + 1.107 \times 10^{-4}T - 8.636 \times 10^{-8}T^2 + 6.314 \times 10^{-11}T^3 - 1.882 \times 10^{-14}T^4$$

Thermal conductivity of solid,  $\lambda_s$ , [ $\text{W}/(\text{m.K})$ ]

$$3.496 + 0.02673T - 1.118 \times 10^{-5}T^2 + 3.607 \times 10^{-9}T^3 + 8.236 \times 10^{-14}T^4$$


---

#### 4. NUMERICAL RESULTS

The cooling effectiveness of the turbine blade with two different inlet injections on the trailing edge is investigated in the present study. The local cooling effectiveness is calculated from the local temperature using the following equation:

$$\eta = \frac{T - T_{\infty}}{T_c - T_{\infty}}. \quad (10)$$

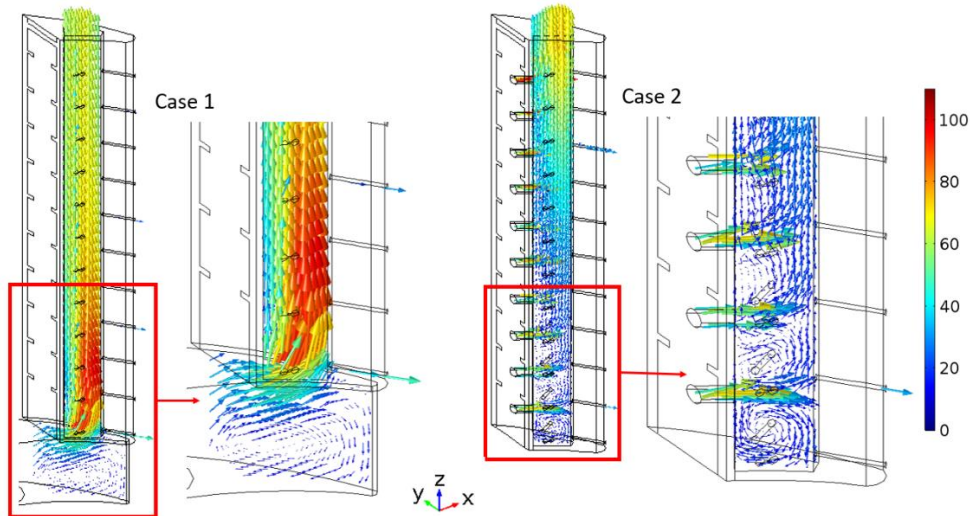


Fig. 3 Velocity flow on the trailing edge coloured by its magnitude (m/s)

Fig. 3 shows the velocity flow on the trailing edge. It is seen that the main flow is generating a big vortex on the bottom in Case 1 and then passing through the trailing edge cavity directly up to the outlet. In Case 2, incoming air flow passing through the first three holes from the bottom to the trailing edge cavity is generating the smaller vortices and then going up to the outlet. The average velocity magnitude of the air in the trailing edge cavity from Case 1 and 2 are 62.77 and 30.12 m/s, respectively.

The cooling effectiveness on the trailing edge from both cases is shown in Fig. 4. In Case 1, the cooling air passing through the trailing edge from the bottom inlet develops the higher cooling effectiveness near the bottom than that from Case 2. In the opposite way, the cooling air from the lateral inlet in Case 2 develops the higher cooling effectiveness near the channel wall than that from Case 1. The lowest cooling effectiveness is detected at the top of the trailing edge from both cases. The overall average cooling effectiveness on the trailing edge of both cases is 0.26.

Fig. 5 (a) shows planar plot of the inner wall cooling effectiveness on the trailing cavity from pressure side to suction side. The cooling effectiveness distribution is correlated with the cooling air flow as mentioned above. It is higher at the inlet and

lower at the outlet due to the lower level of the velocity magnitude. The different values of the cooling effectiveness from both cases are all positive as seen in Fig. 5 (b). It is meant that the overall cooling effectiveness of Case 1 is higher than that of Case 2.

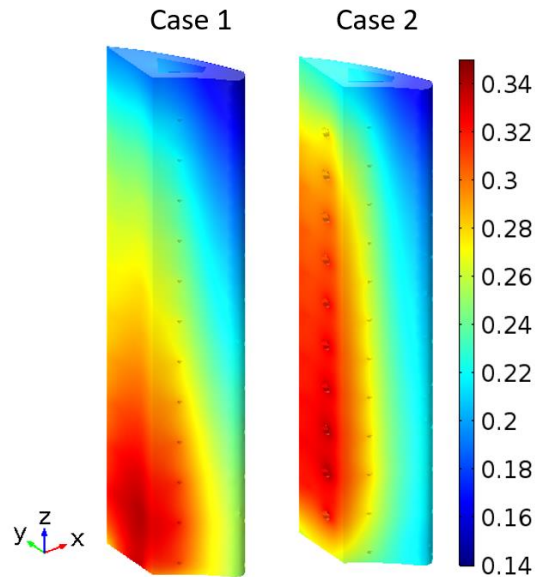


Fig. 4 Cooling effectiveness on the trailing edge

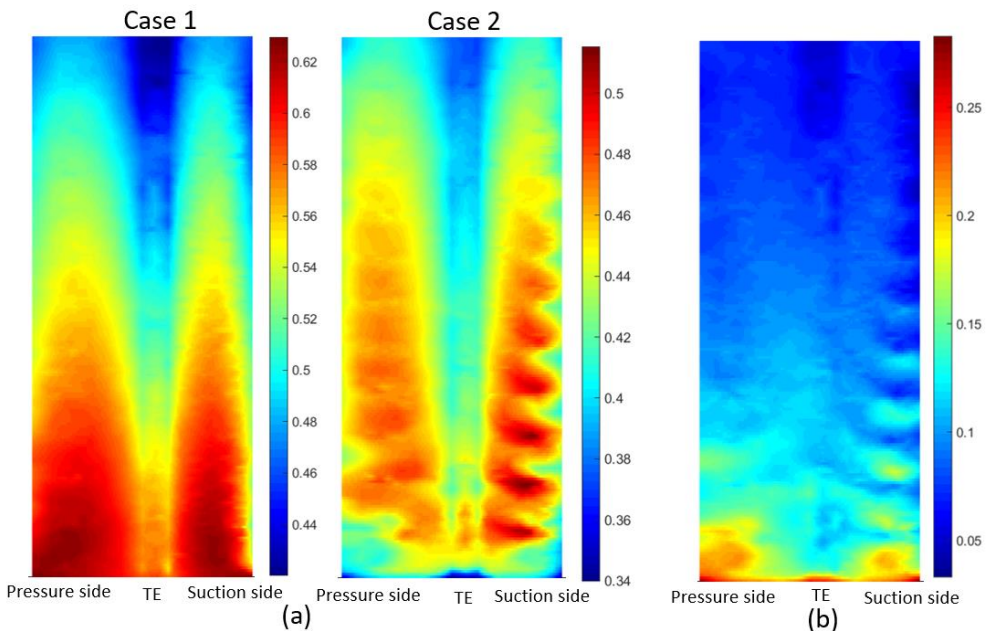


Fig. 5 (a) Inner wall cooling effectiveness (b) difference between the cooling effectiveness of Case 1 and Case 2

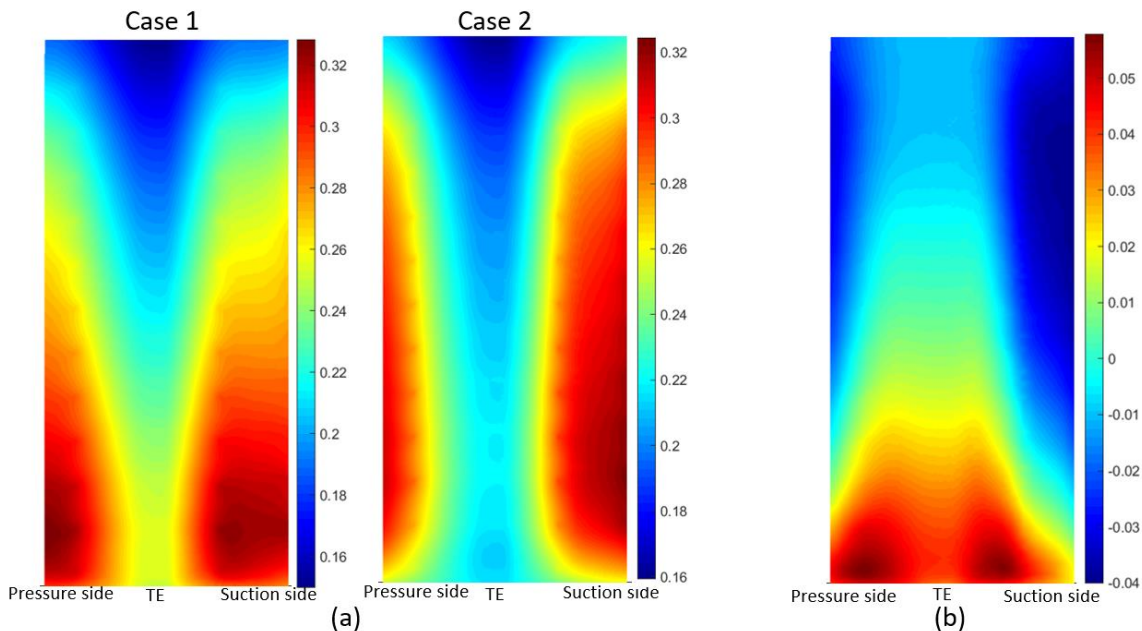


Fig. 6 (a) Surface cooling effectiveness (b) difference between the cooling effectiveness of Case 1 and Case 2

Fig. 6 (a) shows the planar plot of the cooling effectiveness distribution on the surface near the trailing edge from pressure side to suction side. In Case 1, the cooling effectiveness distributes between 0.15 and 0.33. It is higher on the bottom corners and decreases gradually to the top of the trailing edge. In Case 2, the cooling effectiveness is between 0.15 and 0.32. It is higher on the lateral and decreases gradually to the top of the trailing edge. Comparing between two cases, Case 1 has higher level of cooling effectiveness (positive level) on the bottom and lower level (negative level) on the lateral than that of Case 2 as seen in Fig. 6 (b).

## 5. CONCLUSIONS

A steady state three-dimensional mathematical model has been performed to study the turbulence flow and heat transfer in a gas turbine blade. Two different inlet injections on the trailing edge including the bottom inlet and lateral inlet were proposed to investigate the cooling effectiveness. The numerical results obtained from the simulation show that the average velocity magnitude of the bottom inlet case is higher than that of the lateral inlet case. The highest cooling effectiveness on the trailing edge is developed near the inlet hole. It is noted that the lowest cooling effectiveness is at the top of the trailing edge. Therefore, further study will be carried out to increase the cooling effectiveness on the trailing edge.

## REFERENCES

- Becchi, R., Facchini, B., Picchi, A., Tarchi, L., Coutandin, D., and Zecchi, S. (2015), "Film Cooling Adiabatic Effectiveness Measurements of Pressure Side Trailing Edge Cooling Configurations", *Propuls. Power Res.*, **4**(4), 190–201.
- Chung, H., Park, J. S., Sohn, H. S., Rhee, D. H., and Cho, H. H. (2014), "Trailing Edge Cooling of a Gas Turbine Blade with Perforated Blockages with Inclined Holes", *Int. J. Heat Mass Transf.*, **73**, 9–20.
- Cunha, F.J., Dahmer M.T. and Chyu M.K. (2006), "Analysis of Airfoil Trailing Edge Heat Transfer and Its Significance in Thermal-Mechanical Design", *J. Turbomach.*, **128**, 738–46.
- Deng, H., Li, L., Zhu, J., Tao, Z., Tian, S., and Yang, Z. (2018), "Heat Transfer of a Rotating Two-Inlet Trailing Edge Channel with Lateral Fluid Extractions", *Int. J. Therm. Sci.*, **125**, 313–323.
- Effendy, M., Yao, Y. F., Yao, J., and Marchant, D. R. (2016), "DES Study of Blade Trailing Edge Cutback Cooling Performance with Various Lip Thicknesses", *Appl. Therm. Eng.*, **99**, 434–445.
- Kays, W. M. (1994), "Turbulent Pratidtl Number - Where Are We?", *J. Heat Transfer*, **116**(2), 284–295.
- Launder, B. E. and Spalding, D. B. (1974), "The numerical computation of turbulent flows," *Comput. Methods Appl. Mech. Eng.*, **3**(2), 269–289.
- Shen, Z., Xie, Y., and Zhang, D. (2016), "Experimental and Numerical Study on Heat Transfer in Trailing Edge Cooling Passages with Dimples/protrusions under the Effect of Side Wall Slot Ejection", *Int. J. Heat Mass Transf.*, **92**, 1218–1235.
- Siddique, W., Khan, N. A., and Haq, I. (2015), "Analysis of Numerical Results for Two-Pass Trapezoidal Channel with Different Cooling Configurations of Trailing Edge: The Effect of Dimples", *Appl. Therm. Eng.*, **89**, 763–771.
- Taslim, M. E., and Nongsaeng, A. (2011), "Experimental and Numerical Cross-Over Jet Impingement in an Airfoil Trailing-Edge Cooling Channel", *J. Turbomach.*, **133**(4), 41009.
- Taslim, M. E., and Fong, M. K. H. (2013), "Experimental and Numerical Crossover Jet Impingement in a Rib-Roughened Airfoil Trailing-Edge Cooling Channel", *J. Turbomach.*, **135**(5), 51014.
- Yang, Z., and Hu, H., (2012), "An Experimental Investigation on the Trailing Edge Cooling of Turbine Blades", *Propuls. Power Res.*, **1**(1), 36–47.
- Yoshioka, Y., Saito, D. and Ito, S. (1986), "Lifting issues in hot gas path components of heavy-duty gas turbines", *Mater High Temp*, **28**(3), 188–97.